Environmental Health
Engineering and
Management Journal

Original Article

Removal of Acid Orange 7 dye from wastewater using combination of ultraviolet radiation, ultrasonic method, and MgO nanoparticles

Amirreza Talaiekhozani[1]*, Abbas Heydari Chaleshtori[2], Farhad Banisharif[3,4], Zeinab Eskandari[2], Mohammad Nasiri[5], Farham Aminsharei[6,7], Junboum Park[8], Shahabaldin Rezania[9], Maryam Bazrafshan[2]

[1]Department of Civil Engineering, Jami Institute of Technology, Isfahan, Iran
[2]Department of Chemical Engineering, Jami Institute of Technology, Isfahan, Iran
[3]Department of Research and Development, Nirouchlor, Isfahan, Iran
[4]Department Chemical Engineering, School of Chemical, Petroleum and Gas Engineering, Iran University of Science and Technology, Tehran, Iran
[5]Department of Chemistry, Faculty of Applied Science, Malek Ashtar University of Technology, Isfahan, Iran
[6]Department of Safety, Health and Environment, Najafabad Branch, Islamic Azad University, Najafabad, Iran
[7]Human Environment and Sustainable Development Research Center, Najafabad Branch, Islamic Azad University, Najafabad, Iran
[8]Department of Civil and Environmental Engineering, Seoul National University, Seoul, South Korea
[9]Department of Environment and Energy, Sejong University, Seoul, South Korea

Abstract

Background: Industrial dyes are toxic and carcinogenic, therefore, they should be removed from wastewater. The aim of this study was to investigate the removal of acid orange 7 Dye from wastewater using ultraviolet (UV) radiation, MgO nanoparticles, ultrasonic method alone and in combination with each other.

Methods: The effects of some factors such as temperature, pH, hydraulic retention time (HRT), UV power, and concentration of MgO nanoparticles on the removal of Acid Orange 7 dye from synthetic wastewater using different methods were investigated. Also, adsorption isotherms for MgO nanoparticles and kinetics for UV radiation were investigated.

Results: The optimum HRT was 55 minutes while the temperature was not effective in dye removal using the ultrasonic method. Under optimum conditions for UV irradiation method (HRT = 70 minutes, UV power = 170 mW/cm^2, and temperature = 10˚C), 58% of the dye was removed. However, under optimum conditions for MgO nanoparticles method (HRT = 15 minutes, temperature = 20˚C, and ratio of MgO nanoparticles to the initial dye concentration = 67.2), 82% of the dye was removed. By combining these methods, the dye removal efficiency was significantly increased. The combination of ultrasonic method and MgO nanoparticles had no significant effect on increasing the dye removal efficiency from wastewater. It was revealed that dye removal using UV radiation can be described by the first-order kinetics.

Conclusion: According to the results, UV radiation has a synergistic effect on the dye adsorption process by MgO nanoparticles. Therefore, the combination of these methods can be effective for the removal of dye from wastewater.

Keywords: Azo compounds, Ultraviolet rays, Ultrasonic method, Nanoparticles, Waste water, Kinetics

Citation: Talaiekhozani A, Heydari Chaleshtori A, Banisharif F, Eskandari Z, Nasiri M, Aminsharei F, et al. Removal of Acid Orange 7 dye from wastewater using combination of ultraviolet radiation, ultrasonic method, and MgO nanoparticles. Environmental Health Engineering and Management Journal 2019; 6(3): 157–170. doi: 10.15171/EHEM.2019.18.

*Correspondence to:
Amirreza Talaiekhozani
Email: amirtkh@yahoo.com

Introduction

Wastewater from industries such as textile and leather contains residual dyes and is discharged in the environment around industrial area. There are approximately 40 000 various dyes used in industries that azo dyes are the main type of them (1). Over the world, azo dyes account for more than 50% of total dyes used in textile and other industries (2,3). They are toxic and carcinogenic (4). The main part of azo dye is Acid Orange 7 with formula of $C_{16}H_{11}N_2NaO_4S$ (5,6). These dyes escape the wastewater treatment processes and remain in the environment because of their high stability to different parameters such

as light, temperature, water, and detergents (7,8). Several methods have been developed for dye removal from wastewater such as electrochemical methods (4,5), oxidation processes (6), biological degradation (9), UV radiation (8), advanced oxidation processes (8), and adsorption processes (10). Adsorption processes have been reported as the most cost-effective methods for dye removal. In this method, the specific surface area increases with the reduction of particle size (11). By increasing the surface area, the adsorption rate also increases. Many types of adsorbents have been used for the removal of dyes from wastewater (12). Among them, activated carbon is one of the most common adsorbents used to remove dyes, which is an effective material (13). Recently, researchers have focused on the development of new cost-effective adsorbents like nanoparticles for removal of dye from wastewater. Nanoparticles can provide a large specific surface area that make a large fraction of atoms to be more accessible for chemical reactions (14). MgO nanoparticles are very promising adsorbent for dye removal from wastewater (15). The simplicity of MgO nanoparticles production from abundant natural minerals is considered as the main advantage of this adsorbent (12). Recently, ultraviolet (UV) radiation has been also introduced for dye removal from wastewater (16). Studies have shown that the use of UV radiation along with chemical oxidants such as ferrate(VI) can increase the pollutants removal efficiency from wastewater (17). Additionally, UV irradiation could be used for the removal of some organic compounds and hydrogen sulfide (H_2S) from domestic wastewater (18). Another method introduced for dye removal is the use of ultrasonic waves. Ultrasound waves are divided into two categories according to their application: The first category contains ultrasound waves with frequencies between 20 kHz and 1 MHz which are using in chemical processes (19). The second category is ultrasound waves with frequencies less than 1 MHz which are using in medical science (20). The penetration of ultrasonic waves in the aquatic environment is very high that is usually from 15 to 20 cm. The use of ultrasonic waves for chemical reactions is called sonolysis. Sonolysis is an advanced oxidation process that has gained a lot of attention over the past two decades (21).

Although, different methods such as UV radiation (22), electrochemical methods (4), oxidation processes (6), biological degradation (7), ultrasonic waves (19), and adsorption processes (10) have been proposed to remove Acid Orange 7 dye from water, but there is no study about simultaneous application of ultraviolet (UV) + MgO nanoparticles and ultrasonic method + MgO nanoparticles. Therefore, the aims of this study were to investigate the removal of Acid Orange 7 using ultraviolet (UV), MgO nanoparticles, ultrasonic method, UV + MgO nanoparticles, and ultrasonic method + MgO nanoparticles, and to evaluate the effective factors in the removal of Acid Orange 7 from wastewater using above-mentioned methods.

Materials and Methods

Ultrasound

To prepare dye concentration of 11.9 mg/L, 1.19 mg of Acid Orange 7 dye was added into an Erlenmeyer flask containing 100 mL of distilled water. In the previous study (1), it was shown that there is no significant difference in the removal efficiency of different dyes between high and low initial dye concentration. So, it was decided to use only low concentration of the dye. Then, the Erlenmeyer flask was radiated with ultrasonic equipment (S30H) for 60 minutes at 20°C. Sampling was performed every 5 minutes from the Erlenmeyer flask and continued up to 60 minutes. The concentration of the remaining dye in each sample was measured. Then, the effect of different temperatures of 10, 20, 30, 40, 50, and 60°C was evaluated to find the best temperature for the dye removal.

Ultraviolet

In this method, containers with dimensions of 20 × 12 × 2.5 cm were used. UV with a power of 10, 20, 70, 120, and 170 mW/cm² was used to find the effect of UV power on the dye removal. The dye concentration of 11.9 mg/L was selected for this section of the study. Also, the effect of hydraulic retention time (HRT) on dye removal in the range of 1 to 80 minutes was investigated. Then, the effect of different temperatures of 10, 20, 30, 40, 50, and 60°C on dye removal was evaluated.

It should be noted that the investigation of the reaction kinetics is essential to provide the necessary data for the industrial applications of UV radiation. In this study, first-, second-, pseudo first-, and pseudo second-order kinetics for dye removal by UV radiation were investigated. So, first- and second-order kinetics were investigated using equations (1) and (2), respectively.

$$\frac{\ln C_A}{C_{A0}} = -k_1 t \qquad (1)$$

where C_A is the concentration of dye after the treatment by UV radiation (mg/L), C_{A0} is the initial concentration of dye before the treatment by UV radiation (mg/L), and k_1 is the reaction rate constant of the first-order kinetics (1/min). Equation (1) is analogous of $y = ax$ equation. Therefore, k_1 coefficient can be calculated by plotting ln C_A/C_{A0} versus t. Second-order kinetic was evaluated using Eq. (2).

$$\frac{1}{C_A} = k_2 t + \frac{1}{C_{A0}} \qquad (2)$$

Where C_{Ao} is the initial concentration of pollutants (mg/L), C_A is pollutant concentration at time of t (mg/L). k_2 can be calculated by plotting of $1/C_A$ versus t. In this study, pseudo first-order and pseudo second-order kinetics were also investigated that are shown in equations (3) and (4).

$$log (CA \ max - CA) = log (C_{A \ max} - k_1 \times t) \qquad (3)$$

$$\frac{t}{C} = \frac{t}{k_2 \times C_{max}^2} + \frac{t}{C_{max}} \qquad (4)$$

where C is the concentration of dye removal at t (mg/L), C_{max} is the maximum concentration of dye removal (mg/L), k_1 is pseudo first-order reaction rate constants (min^{-1}), and k_2 is pseudo second-order reaction rate constants in L/mg.min (23).

MgO nanoparticles

In this method, the effect of MgO nanoparticles at different concentrations of 10, 20, 30, 40, 50, 60, 70, 80, 90, and 100 mg was investigated. In addition, the effect of temperature in the range of 1 to 25 minutes and different HRTs of 20, 30, 40, 50, and 60°C on dye removal was investigated. Also, isotherms of Freundlich, Langmuir, D-R, Temkin, Generalized, and Jovanovic were studied. The linearized form of Freundlich isotherm is shown in Eq. (5).

$$log \left(\frac{x}{m}\right) = logK_f + \frac{1}{n} log(C_e) \qquad (5)$$

where x/m is the amount of dye absorbed per gram of the absorbent, C_e is the equilibrium concentration of the adsorbed dye in the solution after adsorption process, and n and K_f are the constant coefficients of the Freundlich equation. Equation (6) is similar to the general equation of a straight line ($y=ax+b$). The amount of K_f and n can be calculated by plotting $log(x/m)$ versus $log(C_e)$. Langmuir isotherm is shown in Eq. (6).

$$\frac{C_e}{(x/m)} = \frac{1}{ab} + \frac{1}{a} C_e \qquad (6)$$

where a and b are Langmuir constants. This equation is similar to the general equation of a straight line ($y=ax+b$). The constants a and b can be determined by plotting $C_e/(x/m)$ versus C_e. The Temkin isotherm is shown in Eq. (7). The constants K_T and B_1 can be calculated using the linear plot of q_e versus ln (C_e).

$$q_e = B_1 \ln(K_T) + B_1 \ln(C_e) \qquad (7)$$

Where K_T is the equilibrium binding constant (L/mg) and constant B_1 is the heat of adsorption (21). The D-R isotherm, apart from being analogue of Langmuir isotherm, is more general than Langmuir isotherm as it rejects the homogenous surface or constant adsorption potential. The D-R isotherm is shown in Eq. (8).

$$lnq_e = lnq_s - B\varepsilon^2 \qquad (9)$$

where q_e is D-R constant and ε can be calculated using Eq. (9).

$$\varepsilon = RTln \left(1 + \frac{1}{C_e}\right) \qquad (10)$$

where q_e is the maximum amount of adsorbent that can be adsorbed on the adsorbent, B is the constant related to energy, C_e is the equilibrium concentration (mg/L), R is the universal gas constant that is equal to 8.314 J/mol.K, and T is the temperature (Kelvin). The Generalized isotherm is shown in Eq. (10).

$$ln\left[\left(\frac{q_{max}}{q_e}\right) - 1\right] = ln(K_G) - Nln(C_e) \qquad (10)$$

where K_G is the saturation constant (mg/L), N is the cooperative binding constant, q_{max} is the maximum adsorption capacity of the adsorbent (mg/g), and q_e (mg/g) and C_e (mg/L) are the equilibrium dye concentrations in the soil and liquid phase, respectively. The values of N and K_G were calculated from the slope and intercept of the plots.

Assumptions of the Langmuir model were used to develop Jovanovic isotherm. In addition to the assumptions of the Langmuir model, the possibility of some mechanical contacts between the adsorbate and adsorbent was also considered as a new assumption for Jovanovic isotherm. The linear form of the Jovanovic model is shown in Eq. (11).

$$lnq_e = lnq_{max} - K_J C_e \qquad (11)$$

where C_e is the equilibrium concentration (mg/L), K_J is a constant coefficient of Jovanovic, q_e is the amount of adsorbate that was adsorbed onto the adsorbent at equilibrium stage (mg/g), and q_{max} is the maximum uptake of adsorbate obtained from the plot of lnq_e versus C_e.

Combination of ultrasonic method and MgO nanoparticles

In this method, 10 Erlenmeyer flask with a volume of 2000 mL containing 1000 mL of distilled water and 11.9 mg of Acid Orange 7 were used. Then, different concentrations (200, 300, 400, 500, 600, 700, 800, 900, and 1000 mg) of MgO nanoparticles were added to the Erlenmeyer flasks. Next, the Erlenmeyer flasks were preserved in the ultrasonic equipment at temperature of 23°C for 50 minutes. To determine dye concentration, sampling was performed from each Erlenmeyer flask at 5-minute intervals.

The combination of UV and MgO nanoparticles

In this method, 9 UV containers with 100 mL of distilled water and 11.9 mg/L of dye were prepared. Next, MgO nanoparticles with concentrations between 200 and 1000 mg/L were prepared in the containers. Then, the containers were exposed to UV radiation with a power of 170 mW/cm^2 at temperature of 23°C for 100 minutes. Every 5 minutes, a sample was taken from each container to determine the dye concentration.

MgO nanoparticles generation

Nanoparticles are typically produced by sol-gel and

hydrothermal methods. In this study, sol-gel method was used to produce MgO nanoparticles by adding 100 g of $MgCl_2.6H_2O$ and 50 mL of sodium hydroxide 1 N to 500 mL distilled water. The solution was mixed using magnetic stirrer at 200 rpm for 4 hours. After sedimentation and precipitation, the sediments were separated from the solution by centrifuging at 3000 rpm for 5 minutes. The separated sediments were washed with distilled water several times and dried at 60°C for 24 hours. To obtain MgO nanoparticles, the dried powder was calcined at 450°C for 2 hours. The production of nanoparticles and their dimensions were determined using scanning electron microscope (SEM). The specific surface area of MgO nanoparticles was measured using the Brunauer–Emmett–Teller (BET) equation applied to the adsorption data (24). Also, the pattern of MgO particles was determined using X-ray diffraction (XRD).

Analytical methods

In this study, ferrate(VI) was electrochemically produced based on the study of Talaiekhozani et al (18). All other chemicals were purchased from Merck (Darmstadt, Germany). pH was determined using a digital pH meter (AZ-86502, Taiwan). The UV lamp was 8 Watt and manufactured in Italy. To measure UV power, a UV meter (340A model, Taiwan) was used. The temperature was measured using a digital thermometer (ZH-08 model, China). The Acid Orange 7 dye was measured using a spectrophotometer (Unico S-2100 SUV, USA) at a wavelength of 488 nm. The dye powder was dissolved into water, and then, the absorption of dye solution was spectrophotometrically measured at a wide range of wavelengths (between 200 and 1000 nm). The highest absorption was observed at 488 nm. Consequently, this wavelength was selected to measure dye concentration. The dye removal efficiency in all experiments was determined using Eq. (12).

$$RE = \frac{C_1 - C_2}{C_1} \times 100 \tag{12}$$

where RE is dye removal efficiency (%), C_1 is the initial dye concentration (mg/L), and C_2 is the concentration of dye after treatment. In this study, all experiments were replicated to assure the repeatability of the results. The characteristics of MgO nanoparticles generated in this study were investigated by a SEM (Philips XRD, PW1830 X). Also, the morphology of the generated MgO nanoparticles was evaluated by SEM (Philips XI30). Additionally, the specific surface of the generated MgO was measured using a BET analyzer (F-Sorb X400CE).

Results

Ultrasonic method

In this study, the effect of HRT and temperature on dye removal using ultrasonic method was investigated. It was revealed that HRT between 20 and 55 minutes was effective in dye removal using ultrasonic method (Figure 1a). The maximum dye removal at the optimum HRT was only 19%. However, temperature was not an effective factor in dye removal using ultrasonic method (Figure 1b).

UV radiation

The power of UV radiation between 10 and 170 mW/cm² was effective in dye removal using UV radiation (Figure 2a). It was revealed that the increase of HRT has a positive effect on dye removal using UV radiation (Figure 2b). The increase of temperature has a very negative effect on dye removal (Figure 3). The highest dye removal was obtained at temperature of 10°C. The maximum dye removal using UV radiation was around 58% under optimum conditions (HRT = 70 minutes, pH = 6.5, initial dye concentration = 11.9 mg/L, power of UV radiation = 170 mW/cm², and temperature = 10°C). In this study, the reaction kinetics of dye removal using UV radiation was investigated (Figure 4). The results showed that dye removal using UV radiation can be described by the first-order kinetics (R^2 = 0.947).

In the photocatalysis process, the light photons such as UV radiation are used to produce hydroxyl radical group. The generated hydroxyl radicals attack the dyes and degrade it. It includes band to band excitation of semiconductor particles by irradiation, to generate OH· radicals. If the catalyst is used, the production of radical is accelerated
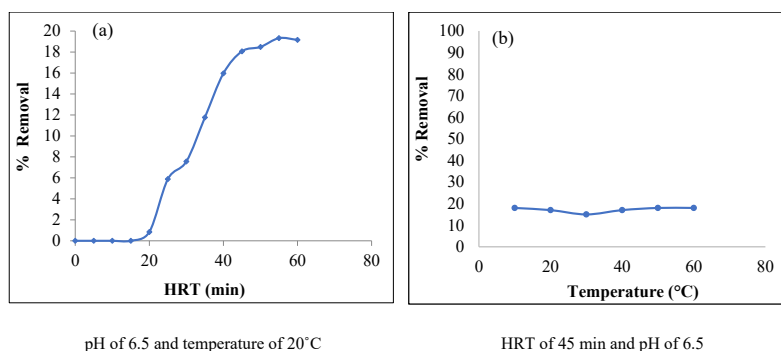

pH of 6.5 and temperature of 20°C   HRT of 45 min and pH of 6.5

Figure 1. The effect of HRT and temperature on dye removal efficiency using ultrasonic method.
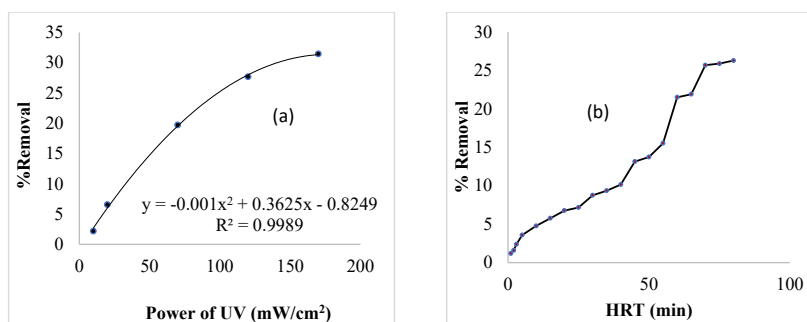
Figure 2. (a) The effect of UV power on removal efficiency of Acid Orange 7 at HRT = 70 min, temperature = 23°C, initial dye concentration = 11.9 mg/L, and pH = 6.5, and (b) The effect of HRT on dye removal using UV radiation at temperature = 23°C, pH = 6.5, initial dye concentration = 11.9 mg/L, and power of UV radiation = 170 mW/cm².
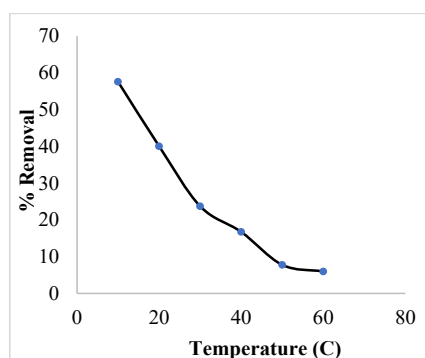

Figure 3. The effect of temperature on dye removal using UV radiation at HRT = 70 min, pH = 6.5, initial dye concentration = 11.9 mg/L, and power of UV radiation = 170 mW/cm².

on the surface of the catalyst. The hydroxyl radical on the particle surface is derived from the valence band hole oxidation of terminal -OH groups and hydration water. It can be assumed that the hydroxyl radical can attack the dual band between nitrogen and degrade the organic dye (2).

Based on the previous work (3), it can be stated that the degradation mechanism was proposed from the initial step of generation of hydroxyl radical to the final product of photocatalytic degradation. It was shown that the dye degradation can be continued via partial or complete oxidation of the naphthalene ring in the structure of Acid Red 7 to form stable intermediates. The OH• radicals attack on the ortho section of naphthalene. Besides,
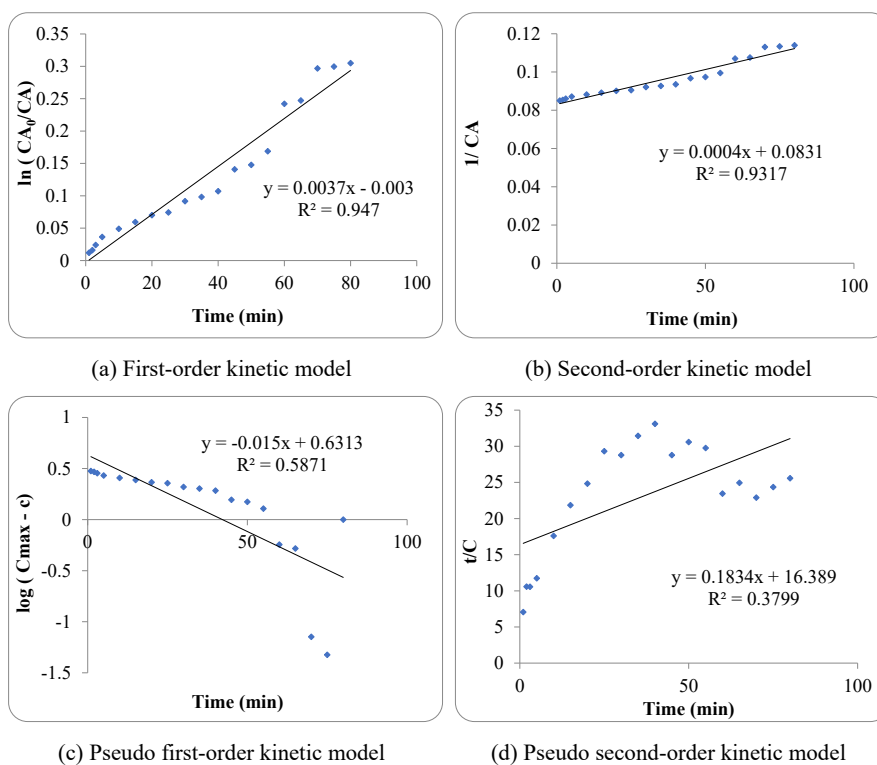

Figure 4. Kinetic investigation for dye removal by UV radiation.

concerted cleavage of the naphthalene ring was resulted in the formation of carboxylic acids.

MgO nanoparticles

The characterestics of syntesized MgO nanoparticles were investigated using SEM and XRD. The size of MgO nanoparticles was investigated by Scherrer equation ($\tau = (K\lambda/\beta cos\theta)$), where τ is the avarage size of particles, K is a dimensionless shape factor, λ is X-ray wavelength, and β is the line broadening at half of the maximum intensity. The investigations using both SEM image and Scherrer equation demonestrated that the avarage size of MgO nanoparticles was between 37 and 73 nm. It was also found that the MgO nanoparticles are almost sphere-shaped (Figure 5a). The results are presented in Figure 5. The effects of the ratio of MgO nanoparticles to the initial dye concentration (M/D) is illustrated in Figure 6a. As shown in this figure, the increase of M/D up to 67 could be effective on dye removal. When M/D was as much as 67, 81% of the dye was removed. The increase of M/D to more than 67 could not increase the dye removal performance. Additionally, HRT between 1 and 10 min was another effective factor on dye removal using MgO nanoparticles (Figure 6b). As temperature has been introduced as an effective factor on adsorption processes, therefore, the effect of this parameter was also investigated on dye removal using MgO nanoparticles. The results demonestrated that the increase of temperature had a negetive effect on dye removal using MgO nanoparticles
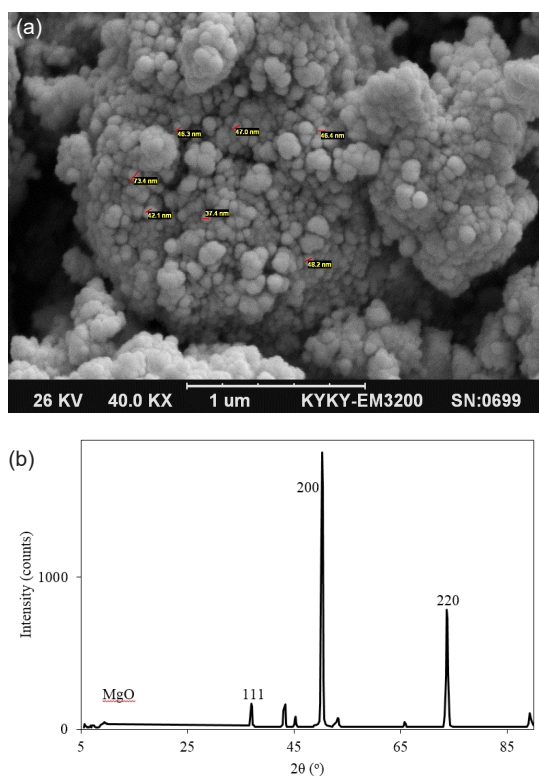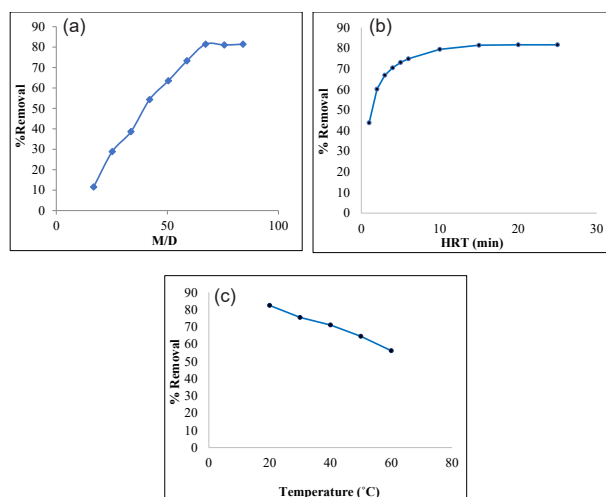

Figure 6. (a) The effect of MgO nanoparticles concentration on dye removal at HRT = 15 min, temperature = 23°C, and pH = 6.5, (b) The effect of HRT on dye removal using MgO nanoparticles at temperature = 23°C, pH = 6.5, and M/D = 58.8, and (c) The effect of temperature on dye removal using MgO nanoparticles at pH = 6.5, HRT = 10 min, and M/D = 58.8.

(Figure 6c). The performance of dye removal using MgO nanoparticles was reduced to 33% at temperature of 60°C in comparison with that at 20°C. Therefore, the use of MgO nanoparticles for dye removal does not need any extera energy for increasing the temperature. As shown in Figure 7, the R^2 of the Langmuir isotherm was greater than that of other isotherm models. It means that the removal of dye from water using MgO nanoparticles can be described by the Langmuir isotherm.

Ultrasonic method + MgO nanoparticles and UV + MgO nanoparticles

The combinations of ultrasonic method + MgO nanoparticles and UV + MgO nanoparticles were investigated in this study. The results of these experiments are shown in Figure 8. Based on Figure 8a, the maximum dye removal using ultrasonic method + MgO nanoparticles process was achieved at HRT of 50 min and M/D of 58.8 (Figure 8a). In this condition, nearly 85% of the dye could be removed. Furthermore, UV/MgO nanoparticles could remove 98% of the dye at HRT of 100 minutes and M/D of 58.8 (Figure 8b). Figure 8c illustrates that the increase of temperature had a positive effect on dye removal using UV/MgO. The results showed that nearly 99% of the dye could be removed at temperature of 60°C and M/D of 16.9 (Figure 8c).

Discussion

Ultrasonic method

Various studies have shown that ultrasonic method can remove various types of pollutants from wastewater (6,25). Based on the results, ultrasonic waves require a long HRT for removal of dye from wastewater (Figure 1a). In this study, the dye was not removed by ultrasonic method in the first 20 min of the experiment. Thereafter,
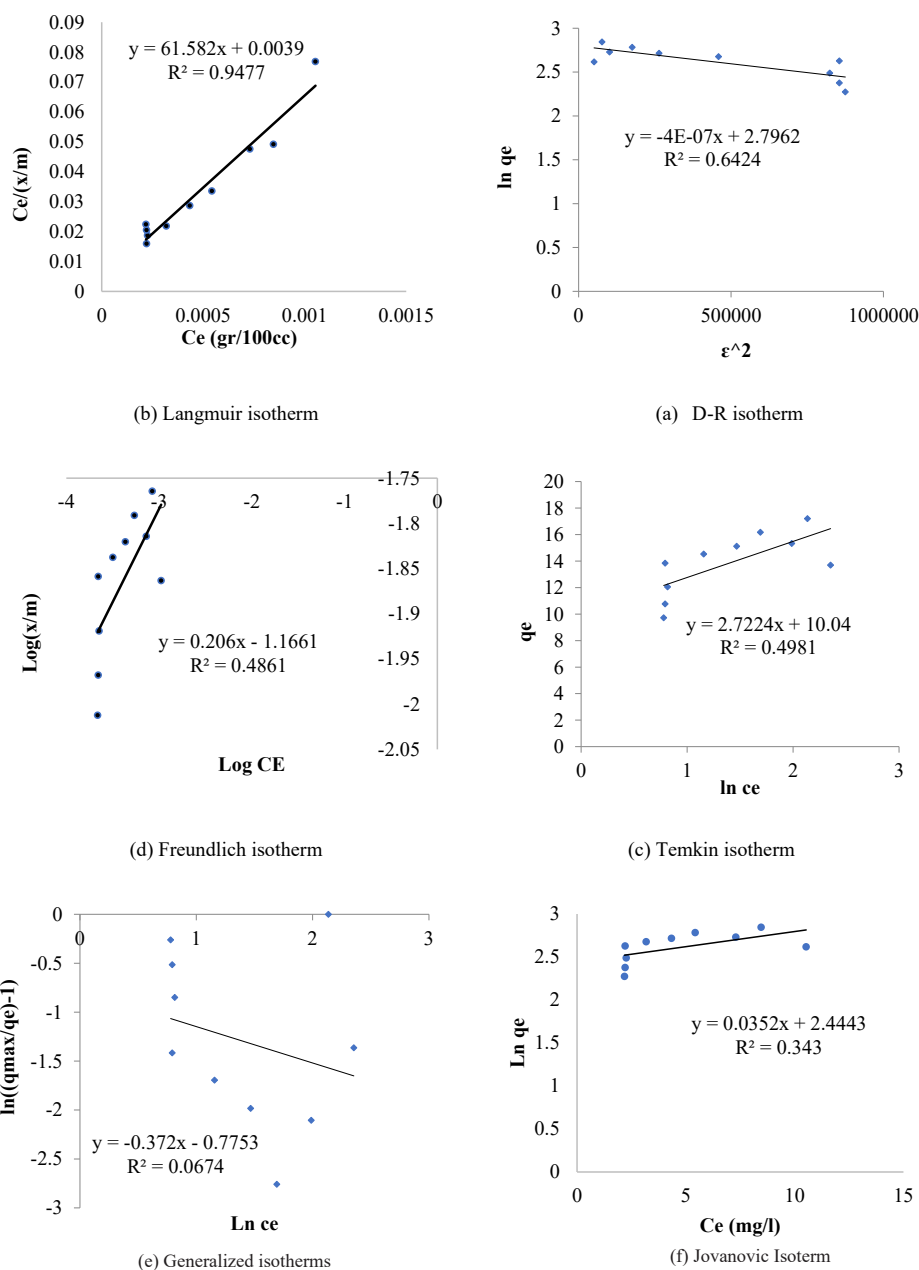

Figure 5. (a) SEM of synthesized MgO nanoparticles and (b) X-RD of synthesized MgO nanoparticles.

(b) Langmuir isotherm

(a) D-R isotherm

(d) Freundlich isotherm

(c) Temkin isotherm

(e) Generalized isotherms

(f) Jovanovic Isoterm

Figure 7. Freundlich, Langmuir, D-R, Temkin, Jovanovic, and Generalized isotherms for removal of dye using MgO nanoparticles.

dye removal efficiency gradually increased to 45 minutes, and then, became stable between 18% and 19%. It can be noted that the ultrasonic method alone was not effective for removal of a large amount of dye from wastewater. As reported by Oh et al, only 21% of the aromatic polycyclic hydrocarbons was removed by the ultrasonic method at HRT of 30 minutes (26).

As temperature is an important parameter in chemical reactions, therefore, the effect of temperature on the ultrasonic method was evaluated. The results showed that dye removal efficiency at different temperatures was stable (Figure 1b). It means that temperature was not an effective factor in dye removal using ultrasonic method.

UV radiation
Effect of UV radiation power
UV radiation with a wavelength between 10 and 400 nm is able to change the chemical nature of many organic compounds (27). The effect of UV power between 10 and 170 mW /cm^2 on the removal of dye from wastewater is shown in Figure 2a. By increasing the power of UV radiation from 10 to 170 mW/cm^2, the removal efficiency increased from 2% to 31%. The relationship between the dye removal efficiency and power of UV radiation can be calculated using Eq. (13).

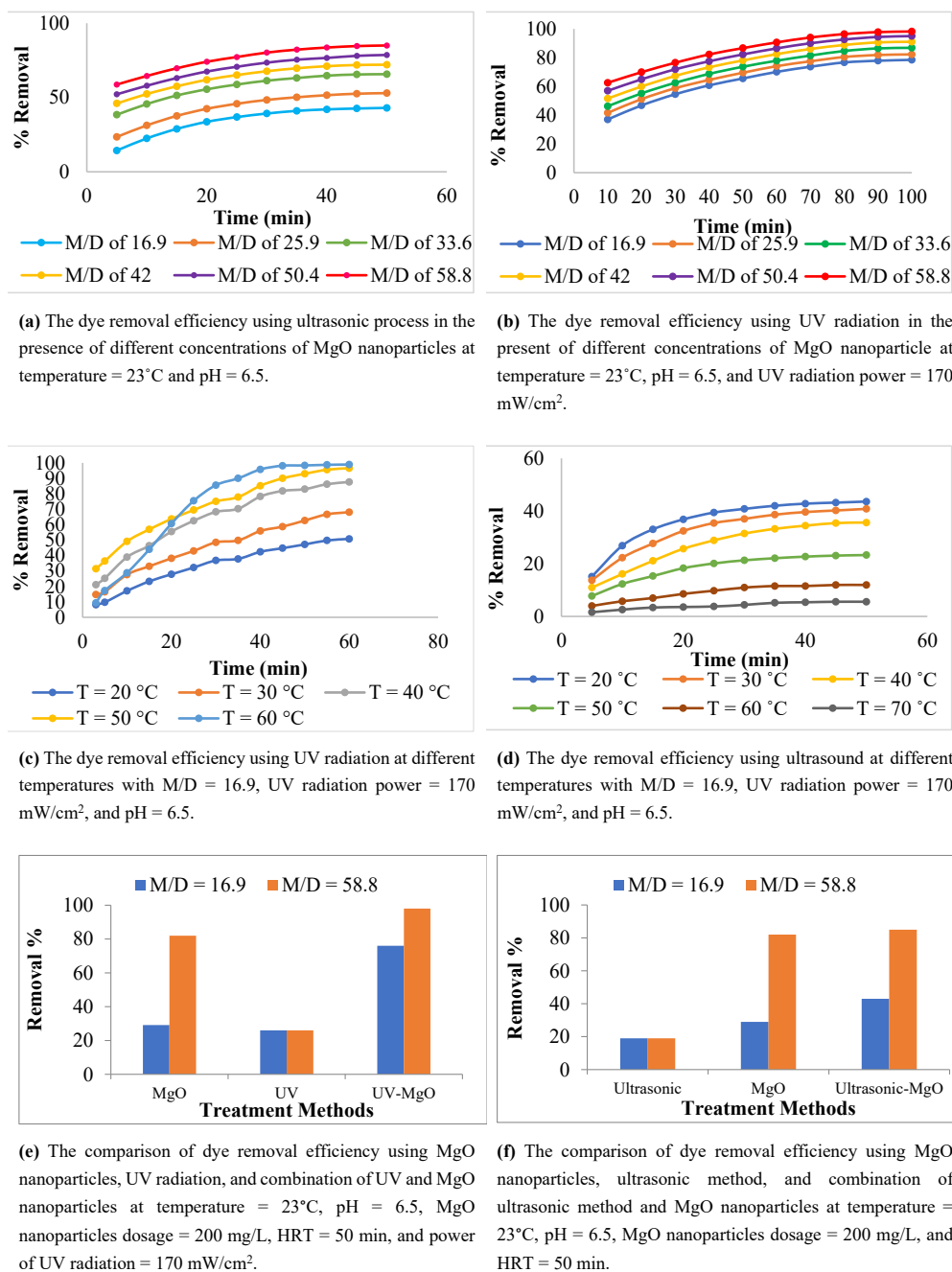$$RE = -0.001(P_{UV})^2 + 0.3625P_{UV} - 0.8249 \qquad (13)$$

(a) The dye removal efficiency using ultrasonic process in the presence of different concentrations of MgO nanoparticles at temperature = 23°C and pH = 6.5.

(b) The dye removal efficiency using UV radiation in the present of different concentrations of MgO nanoparticle at temperature = 23°C, pH = 6.5, and UV radiation power = 170 mW/cm^2.

(c) The dye removal efficiency using UV radiation at different temperatures with M/D = 16.9, UV radiation power = 170 mW/cm^2, and pH = 6.5.

(d) The dye removal efficiency using ultrasound at different temperatures with M/D = 16.9, UV radiation power = 170 mW/cm^2, and pH = 6.5.

(e) The comparison of dye removal efficiency using MgO nanoparticles, UV radiation, and combination of UV and MgO nanoparticles at temperature = 23°C, pH = 6.5, MgO nanoparticles dosage = 200 mg/L, HRT = 50 min, and power of UV radiation = 170 mW/cm^2.

(f) The comparison of dye removal efficiency using MgO nanoparticles, ultrasonic method, and combination of ultrasonic method and MgO nanoparticles at temperature = 23°C, pH = 6.5, MgO nanoparticles dosage = 200 mg/L, and HRT = 50 min.

Figure 8. Comparison of dye removal efficiency using combination of MgO nanoparticles, UV radiation, and ultrasonic method.

where *RE* is the efficiency of dye removal from wastewater (%) and P_{UV} is the power of UV radiation (mW/cm^2). This equation can be used in the range of UV radiation between 10 and 170 mW/cm^2. As reported by Eskandari, about 100% of hydrogen sulfide and 51% of the chemical oxygen demand (COD) were removed from domestic wastewater using UV radiation (17). The results showed that UV radiation alone was not effective in dye removal.

Effect of HRT and temperature

HRT is one of the most important parameters to determine the dimensions of wastewater treatment reactors (28). The results showed that only 1% of the dye was removed at HRT of 1 minute (Figure 2b). By increasing HRT to 70 minutes, the dye removal efficiency increased to 26%. At HRT higher than 70 min, there was no significant change in the removal efficiency of dye from wastewater. The relationship between HRT and the dye removal from wastewater at HRT from 1 to 80 min can be calculated by Eq. (14).

$$RE = 0.3189t + 0.3349 \qquad (R^2 = 0.96) \qquad (14)$$

where *RE* is the removal efficiency of dye from wastewater (%) and *t* is HRT (min). It should be noted that this equation is only applicable at pH = 6.5, temperature =

23°C, and initial Acid Orange 7 dye concentration = 11.9 mg/L.

Figure 3 shows the effect of temperature on dye removal using UV radiation. Based on the results, the increase of temperature had a negative effect on dye removal efficiency using UV radiation. The highest dye removal efficiency was 58% at 10°C. Meanwhile, at a temperature of 50°C, the removal efficiency was decreased to 8%. By increasing the temperature to higher than 50°C, the dye removal efficiency did not change.

Kinetics

In this study, first-, second-, pseudo first-, and pseudo second-order kinetics for dye removal by UV radiation was investigated. Figure 4 shows the regression results of different kinetics. Also, the constant coefficients and relative R^2 are shown in Table 1. The results showed that dye removal using UV radiation can be described by the first-order kinetics (R^2 = 0.947). A first-order reaction depends on the concentration of only one reactant. It means that the dye removal efficiency only depends on the dye concentration. Higher concentration of dye can provide larger molecules that are able to absorb more UV radiation. Therefore, UV radiation is more effective when it is used for removal of dye at higher concentrations. The constant k is the reaction rate constant or reaction rate coefficient, which is shown in 1/min. Its value may depend on conditions such as temperature, ionic strength or light irradiation. The results showed that the reaction rate constant of the first-order kinetics (k_1) was 0.0037 1/min.

MgO nanoparticles

Textural morphology of MgO nanoparticles by SEM image is shown in Figure 5a. Based on the SEM analysis, the size of MgO nanoparticles was found to be between 37 and 75 nm. So, it can be concluded that MgO nanoparticles have been formed well. Figure 5b illustrates the XRD pattern of MgO nanoparticles. Based on the Scherrer equation, the average crystallite size of the particles was around 60 nm. All peaks in the XRD pattern of MgO were very sharp with no impurity, and the crystalline phase was formed completely. Peak intensities in Figure 4b revealed the total scattering from each plane in the phase's crystal structure, which was directly related to the distribution of particular atoms in the structure. The characteristics of diffraction peaks corresponding to crystalline MgO appeared at 2θ = 37.11, 43.0, 50.21 and 73.79°. This pattern showed a single cubic phase that was consistent with those of the standard spectrum (29,30). The results showed that the average specific surface area of MgO nanoparticles was 102.6 m²/g.

Effect of MgO nanoparticles concentration

MgO nanoparticles act as an adsorbent because increasing MgO nanoparticles concentration can increase dye removal efficiency (12). As shown in Figure 6a, M/D increased from 16.9 to 84. By increasing the ratio of M/D from 16.9 to 67.2, the removal efficiency of dye increased. Whereas, increasing the ratio of M/D from 16.9 to 84 did not affect the dye removal efficiency. Increasing the concentration of MgO nanoparticles provides more surfaces for adsorption of dye. However, excessive increase in the absorbent concentration did not increase the dye removal. The results showed that the optimum ratio of M/D to reach the highest dye removal was 67.2. The optimum concentration of MgO nanoparticle for removing Reactive Blue 19 and Reactive Blue 198 dyes at pH = 8, HRT = 5 min, and initial dye concentration between 50 and 300 mg/L, was reported to be 0.2 g (12). Table 2 shows the comparative evaluation of adsorbent dosages removal of dye from wastewater using different adsorbents. The biological oxygen demand (BOD) in wastewater of textile industries before releasing into surface water should be less than 30 mg/L. In this study, after dye removal, the BOD was reduced to 30 mg/L. The

Table 1. The constant coefficients of the first-, second-, pseudo first-, and pseudo second-order kinetics

Pseud First-order Kinetic		Pseudo Second-order Kinetic		First Order Kinetic		Second Order Kinetic	
R^2	k_1 (1/min)	R^2	k_2 (L/mg.min)	R^2	k_1 (1/min)	R^2	k_2 (L/mg.min)
0.5871	0.015	0.3799	0.228837	0.947	0.0037	0.931	0.0004

Table 2. The comparative evaluation of adsorbent dosages for dye removal from wastewater

Adsorbents	Dye Name	Adsorbent Dosage (g/L)	Percentage of Removal (%)	References
Chitosan/Alumina	Methyl Orange	1-12	92-99	(31)
Modified alumina	Crystal violet	5	13-20	(32)
Kaolin	Crystal violet	0.25-4	75-97	(33)
Pine cone	Congo red	0.01-0.03	(32)13-19	(Dawood and Sen, 2012
Fly ash	Methylene blue	8-20	45-96	(34)
Tea waste	Basic yellow 2	2-20	2-20	(35)
MgO nanoparticles	Acid Orange 7	0.1-1	81	Current study

optimum amount of MgO nanoparticles for dye removal was 0.7 g/L. The cost of one kg of MgO nanoparticles is US$ 2560, therefore, it is estimated that the cost of dye removal will be US$ 0.148 per mg of dye.

Effect of HRT and temperature

According to the results, the increase of HRT in the range of 1 to 10 min had a significant effect on the dye removal efficiency using MgO nanoparticles (Figure 6b). Increasing HRT to more than 10 minutes, did not have a significant effect on dye removal. Therefore, the optimum HRT for removal of dye using MgO nanoparticles was determined to be 10 minutes.

Figure 6c shows the effect of temperature on dye removal using MgO nanoparticles. Based on the results, increasing temperature had a negative effect on the dye removal efficiency using MgO nanoparticles. The variations in the removal efficiency of dye in wastewater can be described by the equation $RE = -0.6352T + 95.34$ with a correlation coefficient (R^2) of 0.99, where, RE is dye removal efficiency (%) and T is temperature (°C). Nigam et al reported that by increasing temperature, the removal of dye was slightly decreased when wheat straw, wood chips, and corn-cob shreds were used as the adsorbents. They also reported that 70 to 75% of the dye with an initial concentration of 500 ppm can be removed by corn-cob shreds and wheat straw (36).

If the increase of temperature increases the dye removal efficiency using adsorbent, then, the adsorption is an endothermic process. There are two reasons for this endothermic process behavior: (a) the mobility of dye molecules is increased with increasing temperature and (b) at higher temperatures, the number of active sites in the endothermic adsorbents is increased (37). In contrast, if dye removal efficiency decreases with increasing temperature, the adsorption process is categorized as the exothermic process. The reason for exothermic behavior of adsorbents is the reduction of adsorptive forces between the dye and the active sites on the adsorbent surface (37). The results showed that the adsorption process of MgO nanoparticles is an exothermic adsorption.

Isotherms

The equilibrium adsorption data of Acid Orange 7 onto MgO nanoparticles was analyzed using various isotherm models such as Freundlich, Langmuir, D-R, Temkin, Jovanovic, and Generalized isotherms (Figure 7). All the models were fitted by the equilibrium adsorption data. The best fitted isotherm was introduced based on the values of the R^2 of the linear regression plot. As shown in Figure 7, the R^2 of the Langmuir isotherm was greater than that of other isotherm models. This indicates that the adsorption of dye on the MgO nanoparticles was better described by the Langmuir model in comparison to the other models. In addition, adsorption occurs as the monolayer dyes are adsorbed onto the homogeneous adsorbent surface. The parameter of a in Langmuir isotherm, indicating the adsorption capacity was equal to 0.016 mg/g. The separation factor (S.F.) was calculated using Eq. (15) (38).

$$S.F. = \frac{1}{1 + K_L C_o} \qquad (15)$$

where C_o is the initial dye concentration (mg.L^{-1}) and K_L is the affinity of the binding sites. The S.F. was estimated to be 0.005. So, it can be concluded that the adsorption is favorable because its values were between zero and one (39). Table 3 shows different isotherm results of dye removal by various adsorbents. As can be seen in this table, Langmuir and Freundlich isotherms are the most commonly used isotherms to describe the dyes adsorption process on the adsorbents.

Nanoparticles removal from treated wastewater

The separation of nanoparticles from treated wastewater is a serious challenge. There is no effective way for the removal and disposal of MgO nanoparticle from treated wastewater. Several studies investigated the fate of nanoparticles during wastewater treatment processes (48-53). The product safety data sheet of MgO nanoparticles recommend that it should be dissolved or mixed with a

Table 3. The results of different isotherm studies on dye removal using various adsorbents

Type of Adsorbents	Dye Name	Isotherm Model	References
Chitosan	Congo Red	Langmuir	(40)
Poplar leaf	Methylene blue	Langmuir	(41)
Green alga Chlorella vulgaris	Remazol black	Langmuir	(42)
Chitosan	Methylene blue	Freundlich	(43)
Chitosan	Reactive blue 19	Redlich-Peterson	(44)
Pine leaves	Methylene blue	Langmuir and Freundlich	(44)
Pine leaves	Basic red 46	Langmuir	(45)
Pine cone	Methylene blue	Langmuir	(46)
Activated pine cone	Congo red	Freundlich	(47)
Green alga Chlorella vulgaris	Remazol black	Langmuir	(42)
MgO nanoparticles	Acid orange 7	Langmuir	Current study

combustible solvent and burn in a chemical incinerator, equipped with an afterburner and scrubber. However, it seems that incinerator cannot work for a large amount of treated wastewater. Hou et al found that only about 10% of nanoparticles can be removed from wastewater treatment plants during primary clarification (54). They also reported that during sequencing batch reactor (SBR) processes, some particular nanoparticles were effectively removed in each cycle. It was reported that majority of the oxide nanoparticles could be removed from wastewater by adhesion to clearing sludge or coagulation process (49). Kiser et al found that majority of the nanoparticles larger than 0.7 μm was removed from wastewater treatment using biological methods such as activated sludge (51). Although many studies have been carried out on the removal of nanoparticles from wastewater, the behavior of nanoparticles in wastewater treatment plants is still unknown. Therefore, this field of research is known as one of the major knowledge gaps for accurate environmental risk assessments of nanomaterials (55).

Ultrasonic method + MgO nanoparticles and UV + MgO nanoparticles

Combining different wastewater treatment methods may increase the removal efficiency of pollutants (56,57). Several studies have investigated the combination of UV radiation with other methods to increase the removal efficiency of pollutants since UV radiation alone cannot remove high levels of pollutants (56,58-61). In this study, ultrasonic method and MgO nanoparticles were simultaneously used to remove dye from wastewater. Increasing the M/D ratio increased the removal efficiency of dye from wastewater (Figure 8a). Based on the results, by increasing the HRT to 35 min, dye removal significantly increased when MgO nanoparticles have been used alone. Hence, the combination of ultrasonic method and MgO nanoparticles was not much effective in increasing the dye removal efficiency. Whereas, 60% and 85% of dye were removed at HRTs of 10 and 50 minutes, when the combination of ultrasonic method and MgO nanoparticles was used.

Besides, the combination of UV radiation and MgO nanoparticles was also investigated in this study. It was revealed that by increasing the concentration of MgO nanoparticles, the dye removal efficiency increased (Figure 8b). This study showed that 81% of the dye was removed using MgO nanoparticles and 58% was removed by UV radiation. However, by combination of UV radiation and MgO nanoparticles, 98% of the dye was removed from the wastewater. These results indicate that UV radiation has a synergistic effect on the adsorption performance of the MgO nanoparticles. As shown in Figure 8c, increasing temperature had a positive effect on dye removal efficiency using combination of UV radiation and MgO nanoparticles. At temperatures between 20 and 60°C, dye removal was the highest at 60°C using

combination of MgO nanoparticles and UV radiation. In addition, at temperature of 60°C, 56% and 6% of the dye were removed using MgO nanoparticles and UV radiation, respectively. The mechanism involved in dye removal by the combination of MgO nanoparticles and UV radiation requires further studies.

Figure 8d shows the dye removal efficiency using ultrasound at different temperatures. As shown in this figure, increasing temperature in the range of 20 to 70°C had a negative effect on the dye removal efficiency. The highest dye removal using the combination of ultrasonic method and MgO nanoparticles occurred at temperature of 20°C.

The comparative evaluation of the MgO nanoparticles, UV radiation, and the combination of MgO nanoparticles and UV radiation is shown in Figure 8e and Figure 8f. As can be seen, the dye removal efficiency using the combination of MgO nanoparticles and UV radiation was two times higher than that obtained using these methods alone. Although, in M/D of 58.8, the dye removal efficiency of MgO nanoparticles and ultrasonic method + MgO nanoparticles were two times higher than that in M/D of 16.9 (Figure 8f). It showed that M/D was not only an important factor to use MgO nanoparticles for dye removal but also it was an important factor in the combination of ultrasonic method and MgO nanoparticles.

Conclusion

In this study, the removal of Acid Orange 7 dye from synthetic wastewater using UV radiation, MgO nanoparticles, ultrasonic method, and the combination of these methods was investigated. Based on the results, by using the ultrasonic method for dye removal, 55 min was identified as the optimum HRT, while temperature was not an effective factor. The optimum conditions for dye removal using UV radiation were HRT of 70 min, UV radiation power of 170 mW/cm^2, and temperature of 10°C. Also, the optimum conditions for dye removal using MgO nanoparticles were the ratio of MgO nanoparticles to the initial dye concentration by 67.2, HRT of 15 min, and the temperature of 20°C. The results of this study showed that UV irradiation and MgO nanoparticles respectively removed 58% and 82% of the dye from the wastewater under optimal conditions. Also, it was found that the combination of ultrasonic method and MgO nanoparticles had no significant effect on increasing the dye removal efficiency from wastewater. By combining these methods, the dye removal efficiency significantly increased up to 98%. Additionally, UV radiation had a synergistic effect on the dye adsorption process by MgO nanoparticles. The results of this study can be used to design and operate small and efficient industrial wastewater treatment systems.

Acknowledgments

financial and logistic supports.

Ethical issues

All authors are aware of, and comply with, best practice in publication ethics especially with regard to authorship (avoidance of guest authorship), dual submission, manipulation of figures, competing interests, and compliance with policies on research ethics. Authors certify that all data collected during the study are presented in this manuscript, the submitted work is original, and no data from the study has been or will be published separately elsewhere.

Competing interests

The authors declare that there is no conflict of interests.

Authors' contribution

All authors were equally involved in the collection, analysis, and interpretation of the data. All authors critically reviewed, refined, and approved the manuscript.

References

1. Panswad T, Luangdilok W. Decolorization of reactive dyes with different molecular structures under different environmental conditions. Water Res 2000; 34(17): 4177-84. doi: 10.1016/S0043-1354(00)00200-1.

2. Hisaindee S, Meetani MA, Rauf MA. Application of LC-MS to the analysis of advanced oxidation process (AOP) degradation of dye products and reaction mechanisms. Trends Analyt Chem 2013; 49: 31-44. doi: 10.1016/j.trac.2013.03.011.

3. Bansal P, Singh D, Sud D. Photocatalytic degradation of azo dye in aqueous TiO2 suspension: Reaction pathway and identification of intermediates products by LC/MS. Sep Purif Technol 2010; 72(3): 357-65. doi: 10.1016/j.seppur.2010.03.005.

4. Brillas E, Martínez-Huitle CA. Decontamination of wastewaters containing synthetic organic dyes by electrochemical methods. An updated review. Applied Catalysis B: Environmental 2015; 166-167: 603-43. doi: 10.1016/j.apcatb.2014.11.016.

5. Nidheesh PV, Zhou M, Oturan MA. An overview on the removal of synthetic dyes from water by electrochemical advanced oxidation processes. Chemosphere 2018; 197: 210-27. doi: 10.1016/j.chemosphere.2017.12.195.

6. Ahmad A, Mohd-Setapar SH, Chuong CS, Khatoon A, Wani WA, Kumar R, et al. Recent advances in new generation dye removal technologies: novel search for approaches to reprocess wastewater. RSC Adv 2015; 5(39): 30801-18. doi: 10.1039/C4RA16959J.

7. Roque-Malherbe RM. Adsorption and Diffusion in Nanoporous Materials. 2nd ed. Boca Raton: CRC Press; 2018.

8. Zuorro A, Lavecchia R. Evaluation of UV/H2O2 advanced oxidation process (AOP) for the degradation of diazo dye Reactive Green 19 in aqueous solution. Desalin Water Treat 2014; 52(7-9): 1571-7. doi: 10.1080/19443994.2013.787553.

9. Bhatia D, Sharma NR, Singh J, Kanwar RS. Biological methods for textile dye removal from wastewater: a review.

10. Yagub MT, Sen TK, Afroze S, Ang HM. Dye and its removal from aqueous solution by adsorption: a review. Adv Colloid Interface Sci 2014; 209: 172-84. doi: 10.1016/j.cis.2014.04.002.

11. Perrich JR. Activated Carbon Adsorption for Wastewater Treatment. Boca Raton: CRC Press; 2017.

12. Moussavi G, Mahmoudi M. Removal of azo and anthraquinone reactive dyes from industrial wastewaters using MgO nanoparticles. J Hazard Mater 2009; 168(2-3): 806-12. doi: 10.1016/j.jhazmat.2009.02.097.

13. Wong S, Ngadi N, Inuwa IM, Hassan O. Recent advances in applications of activated carbon from biowaste for wastewater treatment: a short review. J Clean Prod 2018; 175: 361-75. doi: 10.1016/j.jclepro.2017.12.059.

14. Zare EN, Motahari A, Sillanpää M. Nanoadsorbents based on conducting polymer nanocomposites with main focus on polyaniline and its derivatives for removal of heavy metal ions/dyes: a review. Environ Res 2018; 162: 173-95. doi: 10.1016/j.envres.2017.12.025.

15. Haldorai Y, Shim JJ. An efficient removal of methyl orange dye from aqueous solution by adsorption onto chitosan/MgO composite: a novel reusable adsorbent. Appl Surf Sci 2014; 292: 447-53. doi: 10.1016/j.apsusc.2013.11.158.

16. Talaiekhozani A, Eskandari Z, Bagheri M, Talaie MR. Removal of H2S and COD using UV, ferrate and UV/ferrate from municipal wastewater. J Hum Environ Health Promot 2016; 2(1): 1-8. doi: 10.29252/jhehp.2.1.1.

17. Eskandari Z. Control of hydrogen sulfide and organic compounds in municipal wastewater by using ferrate (VI) produced by electrochemical method [dissertation]. Isfahan: Jami Institute of Technology; 2016. [In Persian].

18. Talaiekhozani A, Eskandari Z, Talaei MR, Salari M. Hydrogen sulfide and organic compounds removal in municipal wastewater using ferrate (VI) and ultraviolet radiation. Environmental Health Engineering and Management Journal 2017; 4(1): 7-14. doi: 10.15171/ehem.2017.02.

19. Yang B, Zuo J, Tang X, Liu F, Yu X, Tang X, et al. Effective ultrasound electrochemical degradation of methylene blue wastewater using a nanocoated electrode. Ultrason Sonochem 2014; 21(4): 1310-7. doi: 10.1016/j.ultsonch.2014.01.008.

20. Flower MA. Webb's Physics of Medical Imaging. 2nd ed. Boca Roton: CRC Press; 2012.

21. Bagal MV, Gogate PR. Wastewater treatment using hybrid treatment schemes based on cavitation and Fenton chemistry: a review. Ultrason Sonochem 2014; 21(1): 1-14. doi: 10.1016/j.ultsonch.2013.07.009.

22. Talaiekhozani A, Banisharif F, Eskandari Z, Talaei MR, Park J, Rezania S. Kinetic investigation of 1,9-dimethyl-methylene blue zinc chloride double salt removal from wastewater using ferrate (VI) and ultraviolet radiation. J King Saud Univ Sci 2018; In Press. doi: 10.1016/j.jksus.2018.04.010.

23. Lin H, Lin Y, Liu L. Treatment of dinitrodiazophenol production wastewater by Fe/C and Fe/Cu internal electrolysis and the COD removal kinetics. J Taiwan Inst Chem Eng 2016; 58: 148-54. doi: 10.1016/j.jtice.2015.06.023.

24. Aramendía MA, Benítez JA, Borau V, Jiménez C, Marinas

Crit Rev Environ Sci Technol 2017; 47(19): 1836-76. doi: 10.1080/10643389.2017.1393263.

JM, Ruiz JR, et al. Characterization of various magnesium oxides by XRD and 1H MAS NMR spectroscopy. J Solid State Chem 1999; 144(1): 25-9. doi: 10.1006/jssc.1998.8089.

25. Wang X, Wang L, Li J, Qiu J, Cai C, Zhang H. Degradation of Acid Orange 7 by persulfate activated with zero valent iron in the presence of ultrasonic irradiation. Sep Purif Technol 2014; 122: 41-6. doi: 10.1016/j.seppur.2013.10.037.

26. Oh JY, Choi SD, Kwon HO, Lee SE. Leaching of polycyclic aromatic hydrocarbons (PAHs) from industrial wastewater sludge by ultrasonic treatment. Ultrason Sonochem 2016; 33: 61-6. doi: 10.1016/j.ultsonch.2016.04.027.

27. Bauer R, Waldner G, Fallmann H, Hager S, Klare M, Krutzler T, et al. The photo-fenton reaction and the TiO2/UV process for waste water treatment – novel developments. Catal Today 1999; 53(1): 131-44. doi: 10.1016/S0920-5861(99)00108-X.

28. Tchobanoglous G, Burton FL, Stensel HD. Wastewater Engineering: Treatment and Reuse. 4th ed. Boston: McGraw Hill; 2003.

29. Samantilleke AP, Rebouta LM, Garim V, Rubio-Peña L, Lanceros-Mendez S, Alpuim P, et al. Cohesive strength of nanocrystalline ZnO: Ga thin films deposited at room temperature. Nanoscale Res Lett 2011; 6(1): 309. doi: 10.1186/1556-276X-6-309.

30. Athar T, Hakeem A, Ahmed W. Synthesis of MgO nanopowder via non aqueous sol–gel method. Adv Sci Lett 2012; 7(1): 27-9. doi: 10.1166/asl.2012.2190.

31. Zhang J, Zhou Q, Ou L. Kinetic, isotherm, and thermodynamic studies of the adsorption of methyl orange from aqueous solution by chitosan/alumina composite. J Chem Eng Data 2012; 57(2): 412-9. doi: 10.1021/je2009945.

32. Dawood S, Sen TK. Removal of anionic dye Congo red from aqueous solution by raw pine and acid-treated pine cone powder as adsorbent: equilibrium, thermodynamic, kinetics, mechanism and process design. Water Res 2012; 46(6): 1933-46. doi: 10.1016/j.watres.2012.01.009.

33. Nandi BK, Goswami A, Das AK, Mondal B, Purkait MK. Kinetic and equilibrium studies on the adsorption of crystal violet dye using kaolin as an adsorbent. Sep Sci Technol 2008; 43(6): 1382-403. doi: 10.1080/01496390701885331.

34. Kumar KV, Ramamurthi V, Sivanesan S. Modeling the mechanism involved during the sorption of methylene blue onto fly ash. J Colloid Interface Sci 2005; 284(1): 14-21. doi: 10.1016/j.jcis.2004.09.063.

35. Khosla E, Kaur S, Dave PN. Tea waste as adsorbent for ionic dyes. Desalin Water Treat 2013; 51(34-36): 6552-61. doi: 10.1080/19443994.2013.791776.

36. Nigam P, Armour G, Banat IM, Singh D, Marchant R. Physical removal of textile dyes from effluents and solid-state fermentation of dye-adsorbed agricultural residues. Bioresour Technol 2000; 72(3): 219-26. doi: 10.1016/S0960-8524(99)00123-6.

37. Salleh MA, Mahmoud DK, Karim WA, Idris A. Cationic and anionic dye adsorption by agricultural solid wastes: A comprehensive review. Desalination 2011; 280(1-3): 1-13. doi: 10.1016/j.desal.2011.07.019.

38. Kaur S, Rani S, Mahajan RK. Adsorption kinetics for the removal of hazardous dye Congo Red by biowaste materials as adsorbents. J Chem 2013; 2013: 628582. doi: 10.1155/2013/628582.

39. Crini G. Kinetic and equilibrium studies on the removal of cationic dyes from aqueous solution by adsorption onto a cyclodextrin polymer. Dyes Pigments 2008; 77(2): 415-26. doi: 10.1016/j.dyepig.2007.07.001.

40. Wang L, Wang A. Adsorption characteristics of Congo Red onto the chitosan/montmorillonite nanocomposite. J Hazard Mater 2007; 147(3): 979-85. doi: 10.1016/j.jhazmat.2007.01.145.

41. Han X, Niu X, Ma X. Adsorption characteristics of methylene blue on poplar leaf in batch mode: Equilibrium, kinetics and thermodynamics. Korean J Chem Eng 2012; 29(4): 494-502. doi: 10.1007/s11814-011-0211-5.

42. Aksu Z, Tezer S. Biosorption of reactive dyes on the green alga . Process Biochemistry 2005; 40(3-4): 1347-61. doi: 10.1016/j.procbio.2004.06.007.

43. Chang MY, Juang RS. Adsorption of tannic acid, humic acid, and dyes from water using the composite of chitosan and activated clay. J Colloid Interface Sci 2004; 278(1): 18-25. doi: 10.1016/j.jcis.2004.05.029.

44. Hasan M, Ahmad AL, Hameed BH. Adsorption of reactive dye onto cross-linked chitosan/oil palm ash composite beads. Chem Eng J 2008; 136(2-3): 164-72. doi: 10.1016/j.cej.2007.03.038.

45. Deniz F, Karaman S. Removal of Basic Red 46 dye from aqueous solution by pine tree leaves. Chem Eng J 2011; 170(1): 67-74. doi: 10.1016/j.cej.2011.03.029.

46. Sen TK. Agricultural by-product biomass for removal of pollutants from aqueous solution by adsorption. J Environ Res Dev 2012; 6(3): 523-33.

47. Ibrahim S, Fatimah I, Ang HM, Wang S. Adsorption of anionic dyes in aqueous solution using chemically modified barley straw. Water Sci Technol 2010; 62(5): 1177-82. doi: 10.2166/wst.2010.388.

48. Chang MR, Lee DJ, Lai JY. Nanoparticles in wastewater from a science-based industrial park—Coagulation using polyaluminum chloride. J Environ Manage 2007; 85(4): 1009-14. doi: 10.1016/j.jenvman.2006.11.013.

49. Limbach LK, Bereiter R, Müller E, Krebs R, Galli R, Stark WJ. Removal of oxide nanoparticles in a model wastewater treatment plant: influence of agglomeration and surfactants on clearing efficiency. Environ Sci Technol 2008; 42(15): 5828-33. doi: 10.1021/es800091f.

50. Jarvie HP, Al-Obaidi H, King SM, Bowes MJ, Lawrence MJ, Drake AF, et al. Fate of silica nanoparticles in simulated primary wastewater treatment. Environ Sci Technol 2009; 43(22): 8622-8. doi: 10.1021/es901399q.

51. Kiser MA, Westerhoff P, Benn T, Wang Y, Pérez-Rivera J, Hristovski K. Titanium nanomaterial removal and release from wastewater treatment plants. Environ Sci Technol 2009; 43(17): 6757-63. doi: 10.1021/es901102n.

52. Ganesh R, Smeraldi J, Hosseini T, Khatib L, Olson BH, Rosso D. Evaluation of nanocopper removal and toxicity in municipal wastewaters. Environ Sci Technol 2010; 44(20): 7808-13. doi: 10.1021/es101355k.

53. Kaegi R, Voegelin A, Sinnet B, Zuleeg S, Hagendorfer H, Burkhardt M, et al. Behavior of metallic silver nanoparticles in a pilot wastewater treatment plant. Environ Sci Technol 2011; 45(9): 3902-8. doi: 10.1021/es1041892.

54. Hou L, Li K, Ding Y, Li Y, Chen J, Wu X, et al. Removal of silver nanoparticles in simulated wastewater treatment processes and its impact on COD and NH4 reduction. Chemosphere 2012; 87(3): 248-52. doi: 10.1016/j.

chemosphere.2011.12.042.

55. Scheringer M. Nanoecotoxicology: environmental risks of nanomaterials. Nat Nanotechnol 2008; 3(6): 322-3. doi: 10.1038/nnano.2008.145.

56. Jorfi S, Barzegar G, Ahmadi M, Darvishi Cheshmeh Soltani R, Alah Jafarzadeh Haghighifard N, Takdastan A, et al. Enhanced coagulation-photocatalytic treatment of Acid red 73 dye and real textile wastewater using UVA/synthesized MgO nanoparticles. J Environ Manage 2016; 177: 111-8. doi: 10.1016/j.jenvman.2016.04.005.

57. Darvishi Cheshmeh Soltani R, Jorfi S, Ramezani H, Purfadakari S. Ultrasonically induced ZnO-biosilica nanocomposite for degradation of a textile dye in aqueous phase. Ultrason Sonochem 2016; 28: 69-78. doi: 10.1016/j.ultsonch.2015.07.002.

58. Liu CC, Hsieh YH, Lai PF, Li CH, Kao CL. Photodegradation treatment of azo dye wastewater by UV/TiO2 process. Dyes Pigments 2006; 68(2-3): 191-5. doi: 10.1016/j.dyepig.2004.12.002.

59. Liu F, Ma BR, Zhou D, Zhu LJ, Fu YY, Xue LX. Positively charged loose nanofiltration membrane grafted by diallyl dimethyl ammonium chloride (DADMAC) via UV for salt and dye removal. React Funct Polym 2015; 86: 191-8. doi: 10.1016/j.reactfunctpolym.2014.09.003.

60. Vaiano V, Sacco O, Sannino D, Ciambelli P. Nanostructured N-doped TiO2 coated on glass spheres for the photocatalytic removal of organic dyes under UV or visible light irradiation. Applied Catalysis B: Environmental 2015; 170-171: 153-61. doi: 10.1016/j.apcatb.2015.01.039.

61. Ahmadi Moghadam M, Jaafarzadeh Haghighifard N, Mirali S, Jorfi S, Dinarvand F, Alavi N. Efficiency study on nanophotocatalytic degradation and detoxification of C.I.direct blue 86 from Aquatic Solution Using UVA/TiO2 and UVA/ZnO. Journal of Mazandaran University of Medical Sciences 2016; 26(143): 145-59. [In Persian].